U. S. Department of Energy

A HYBRID HYDROLOGIC - GEOPHYSICAL INVERSE TECHNIQUE FOR THE ASSESSMENT AND MONITORING OF LEACHATES IN THE VADOSE ZONE

Principle Investigator: David L. Alumbaugh

Formerly Sandia National Laboratories
Currently University of Wisconsin, Madison

James Brainard and Robert Glass

Sandia National Laboratories

T. C. Jim Yeh

University of Arizona

Doug LaBrecque

Formerly University of Arizona
Currently MultiPhase Technologies, LLC

Project Number EMSP-55332

Project Duration: 9/1/96-8/1/00

Table of Contents

1 Executive Summary:

The research conducted under this project has led to the development of a new, integrated Hybrid Hydrologic-Geophysical Inverse Technique (HHGIT) for characterization of the vadose zone at contaminated sites. The HHGIT combines information from geophysical measurements, statistical information about the geologic formations, and sparse data on moisture contents. Combining these three data types provide better estimates of hydraulic properties than could be obtained from the individual data types. This new approach to site characterization and monitoring has the potential to provide detailed knowledge about hydrological properties, geological heterogeneity and the extent and movement of contamination at DOE sites.

Controlled field experiments have been conducted to not only provide critical data sets for development and evaluation of the HHGIT, but to also help better understand the mechanisms controlling contaminant movement in the vadose zone. In addition, the experiments have provided a test bed to determine the accuracy of the geophysically derived estimates of moisture content, and how that error effects the resulting hydrologic interpretation.

2 Research Objectives:

At many DOE facilities, the presence of radioactive wastes and other contaminants within the vadose zone poses a serious and ongoing threat to public health and safety. In many cases these contaminants have been introduced directly to the vadose zone through releases on the surface or in shallow pits, and through leaking storage facilities. To reduce the environmental risks these wastes pose, the DOE is currently considering two fundamentally different approaches. The first involves remediation by treating contaminants in-place while the second, and more economically feasible being examined by DOE, involves in-situ immobilization of the wastes. Immobilization would be achieved through both injection of subsurface grout barriers to block transport pathways and installation of surface caps to prevent additional water infiltration into contaminated formations.

A necessary requirement of both remediation approaches is the need to obtain information on the spatial distributions of the hydraulic and transport properties, the amount of contamination in place, and flow and transport processes that are occurring. With this information in hand, informed decisions can be made in order to optimize the remediation process for each particular case. In particular, these capabilities could result in reduced remediation costs, as well as providing necessary data to illustrate regulatory compliance. To reach these goals, existing monitoring technologies need to be improved and innovative technologies need to be developed to measure the spatial distribution of, and the temporal changes in moisture contents and contaminant concentrations within the vadose zone.

The primary objective of the funded research addressed these needs through the development and field-testing of a Hybrid Hydrologic-Geophysical Inverse Technique (HHGIT). The resulting technology provides the ability to both monitor the evolution of certain types of contaminant plumes, and to characterize hydrologic properties within the vadose zone at contaminated sites. The HHGIT combines geophysical measurements such as electrical resistivity tomography (ERT), cross borehole ground penetrating radar (XBGPR), neutron moisture logs, sparse hydrologic data, and geostatistical information on the geologic heterogeneity to provide 2- and 3-D of moisture and hydrologic property distributions. By linking these three types of information into a single inversion, much better estimates of spatially varying hydraulic properties can be obtained than could be from interpreting the data types individually. Because the method is a geostatistically based estimation technique, the estimates represent conditional mean hydraulic property fields. Thus, this method quantifies the uncertainty of the estimates as well as the estimates themselves.

3 Methods and Results:

3.1 The Sandia-Tech Vadose Zone Facility Infiltration Experiment

3.1.1 Background

The Sandia-Tech Vadose Zone Facility (STVZ) is a state-of-the-art infiltration facility developed specifically to provide hydrologic and geophysical data for developing and evaluating the various components of the HHGIT. The field site is located adjacent to the New Mexico Institute of Mining and Technology campus in Socorro, NM on poorly consolidated, heterogeneous alluvial deposits comprised of inter-bedded sands, gravels, and clays. Key features of the site and the facility include the following:

- The site location provides the opportunity to investigate flow and transport processes in unsaturated deposits exhibiting heterogeneity on scales ranging from micro-structures through small scale cross-bedding to fairly homogenous beds as thick as 7 meters.
- The site is built on a small hill allowing for access to geologic deposits for direct observation and sample collection
- The instrument arrays interrogate a volume approaching that of actual contamination plumes (approximately 3000 cubic meters).
- The infiltrometer is designed to provide an even flux of water over a 3 by 3 meter infiltration surface.
- Gains and loses in subsurface moisture contents arising from precipitation and evaporation are prevented with a impermeable buried tarp extending beyond the surface area above the instrumentation.
- Extensive use of automated data acquisition systems reduces measurement errors and provides temporally dense data sets.

All components of the STVZ facility are designed to provide continuous long-term service. A building at the site provides shelter for the data acquisition equipment and the water supply system. All water supply lines are buried or protected with insulation and heat tape to assure continued operation during cold weather. The infiltrometer is of rugged construction and can withstand high winds. A photograph of the site is given in Figure 1.

3.1.2 Instrumentation

The site is instrumented with arrays of transducer- equipped tensiometers, suction lysimeters, TDR probes, thermocouples, and electrode arrays for collecting ERT data. PVC pipes measuring 2 inches in diameter provide access for down-hole geophysical measurements. All arrays are arranged in an axisymmetric pattern as seen in plan view and cover a 10-m square surface area. The arrays are centered on the 3-m square infiltrometer designed to provide a constant flux of water across the infiltration surface. A plan-view of instrument locations along with identifiers is given in Figure 2.

3.1.3 Geological Characterization

Geologic mapping at the STVZ provided critical geologic information on those features that may control flow and transport processes, that reflect the distribution of hydrologic properties, and that may influence the geophysical measurements. To this end, cuttings from 41 instrumentation boreholes and 4 continuous core samples located axi-symmetrically about the infiltrometer (Figure 2) and drilled to a depths up to 12 m provided the data for developing a stratigraphic model of the deposits. Electromagnetic induction and natural gamma borehole logs from all 41 holes aided in locating and verifying contacts between units of contrasting conductivity and mineralogy, while exposures in two trench 1.5 m deep excavations adjacent to the instrument pad, and a nearby sandpit which exposed the lower, provided additional geologic information. Four simplified stratigraphic columns are depicted in Figure 3, along with the interpreted correlation between mappable geologic units.

3.1.4 Hydrological Characterization

Both forward and inverse hydrologic algorithms rely on parametric equations that describe the relationship between in-situ moisture content and the matric potential, as well as the saturated hydraulic conductivity to perform necessary calculations. Commonly, the parametric equations (Brooks-Corey and van Genuchten) are used in conjunction with theoretical pore-size distribution models (Mualem and Burdine) to predict the unsaturated hydraulic conductivity. To this end, a series of moisture retention curves were measured along with saturated hydraulic conductivity on 24 samples collected from the northwest continuous core (see Figure 2 for location). The moisture retention curves were obtained using hanging column apparatuses, while the saturated hydraulic conductivity measurements employed a constant head permeameter system. These properties were measured following ASTM laboratory procedures.

Figure 1 - View of the STVZ looking to the northwest. The infiltrometer is seen as the white square located amongst large diameter PVC stand pipes covering tensiometer access tubes and smaller diameter PVC access tubes used for neutron and XBGPR logging. The building houses data acquisition and water supply equipment.

3.1.5 Constant Flux Infiltration Experiment

The research objectives of this project required that unsaturated conditions be maintained via infiltration of potable water at a flux rate that is less than the saturated hydraulic conductivity. To meet this objective, an infiltration system supplying intermittent pulses of water to yield a flux of 2.7 cm per day was designed. Water for the experiment is provided by a nearby well. The infiltration event has been ongoing since March of 1999.

Automated data loggers were used to monitor flow. Other measurements taken during the infiltration event include the following.

- Volumetric moisture contents using neutron logs within all 13 PVC cased wells.
- Matric-potentials from pressure-transducer equipped tensiometers.
- Two-dimensional (2-D) moisture content fields along the SW-NE transect indicated in Figure 2 from XBGPR images.

- Three-dimensional (3-D) moisture content fields from the ERT images.

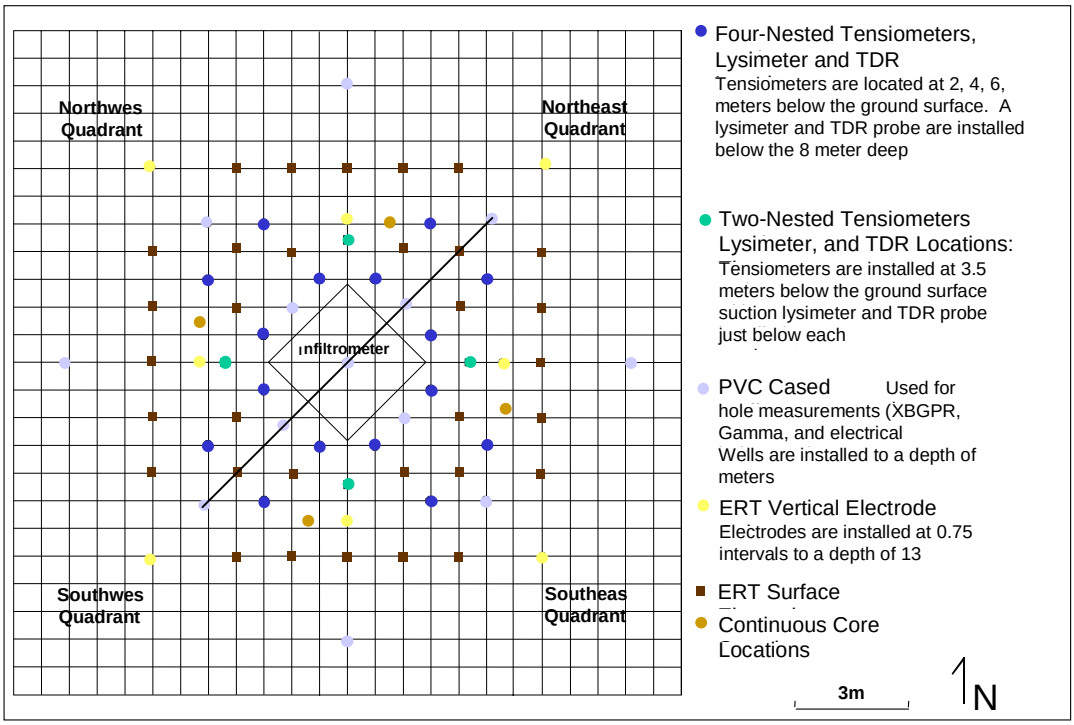

Figure 2: Plan-view schematic of the instrument arrays layout relative to the infiltrometer. The diagonal line running from the Southwest to the Northeast quadrants indicate the transect on which XBGPR readings were taken (See Section 3.3). Not also that ERT electrode locations are also indicated (See Section 3.2).

3.2 Electrical Resistivity Tomography (ERT) Imaging of the Sandia-Tech Vadose Zone (STVZ) Experiment

3.2.1 Background

Electrical resistivity tomography (ERT) is a powerful 3-D monitoring and characterization technology that has recently become popular for environmental applications. ERT is an adaptation of the traditional surface resistivity geophysical method where by a low-frequency electric current is transmitted into the ground via a pair of metal electrodes, while voltages are measured at a second pair of electrodes. By making measurements using a number of different pairs of electrodes, it is possible to infer the resistivity structure of the earth in and below the survey area. For the traditional surface-resistivity method, the resolution decreases rapidly with increasing depth. To circumvent this problem, ERT uses electrodes placed in boreholes as well as on the surface, which provides better resolution of the volume between the boreholes than surface measurements alone. The electrodes are simple and inexpensive enough to be installed permanently within the subsurface, and are emplaced either by attaching them to the outsides of non-metallic cased monitoring wells, or emplacing them in dedicated boreholes or cone-penetrometer holes. Permanent subsurface electrodes provide a very stable platform for making precise comparisons between measurements made at different times.

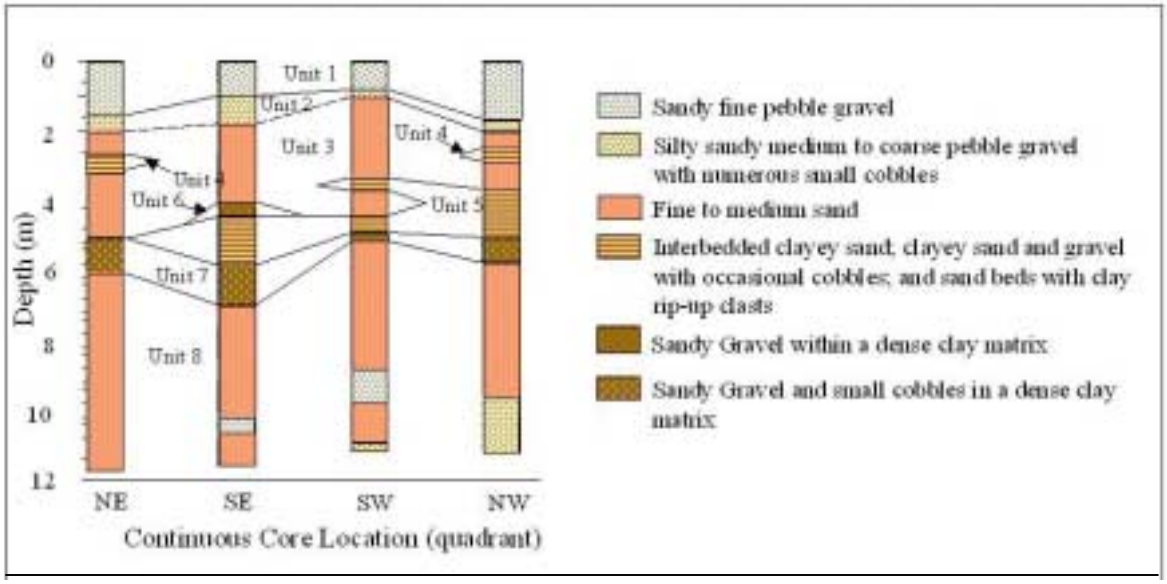

Figure 3: Stratigraphic columns and brief descriptions derived from the four continuos cores extracted from locations in each of the four quadrants depicted in Figure 2. Interpreted correlations between mappable geologic units are also shown.

Due to the sensitivity of soil resistivity to variations in porosity as well as fluid saturation and chemistry, ERT has the potential for wide use in monitoring vadose zone hydrogeologic conditions. For a total of n electrodes, there are n · (n-3)/2 linearly independent measurements; at the STVZ facility each data set contains about 20,000 data points. Because of the large volume of data that is generated, the ERT method requires the use of sophisticated inversion algorithms. It is no surprise then that advancements in ERT have closely followed the development of fast, cheap computers.

3.2.2 The Stochastic ERT Inverse Algorithm

A significant portion of the research effort was focused on developing a new, stochastic inversion method for ERT. The stochastic inversion method (Zhang et al., 1995) seeks to maximize the *a posteriori* probability density function of model parameters. Maximizing *a posteriori* probability density function is equivalent to minimizing the objective function that is given by

$$\mathbf{S(m)} = (\mathbf{g(m)} - \mathbf{d}_{obs})^T \mathbf{C}_D^{-1} (\mathbf{g(m)} - \mathbf{d}_{obs}) + (\mathbf{m} - \mathbf{m}_{prior})^T \mathbf{C}_M^{-1} (\mathbf{m} - \mathbf{m}_{prior}) \qquad (1)$$

where **m** is the model we wish to recover, $\mathbf{d_{obs}}$ is observed data, **g(m)** is a function that relates the model parameters to the measured data, $\mathbf{m}_{\text{prior}}$ is the *a priori* model parameters, $\mathbf{C_D}$ is the data noise covariance matrix, and $\mathbf{C_M}$ is the model parameter covariance matrix (Tarantola ,1987; Yang and LaBrecque, 1999). Minimization of this objective function by Newton's method yields the following iterative algorithm:

$$\mathbf{m}_{n+1} = \mathbf{m}_n - \left(\mathbf{G}_n^T \mathbf{C}_D^{-1} \mathbf{G}_n + \mathbf{C}_M^{-1}\right)^{-1} \cdot \left[\mathbf{G}_n^T \mathbf{C}_D^{-1} \left(\mathbf{g}(\mathbf{m}_n) - \mathbf{d}_{obs}\right) + \mathbf{C}_M^{-1} \left(\mathbf{m}_n - \mathbf{m}_{prior}\right)\right] \qquad (2)$$

where $\mathbf{m}_{n+1}$ is the updated model at iteration n+1, $\mathbf{m}_n$ is model from the previous iteration, and $\mathbf{G}_n$ is the Jacobian, or sensitivity matrix, that relates small perturbations in model parameters to perturbations in the data.

In much of the previous work on stochastic inversion, the parameters are assumed to be uncorrelated. Although this is not a particularly reasonable assumption, it greatly simplifies the computation of the equation above since the resulting covariance matrix is diagonal in which case the

stochastic inversion algorithm is reduced into the damped least squares scheme (Aki and Richards, 1981). One of the innovations in this project was to apply reasonable estimates of the parameter covariance. Because of this, the parameter covariance matrix is "full" and very large, (commonly 80,000 by 80,000 elements). Inversion of this large matrix can be avoided by rearranging the system of equations as:

$$\left(\mathbf{C}_{\mathrm{M}}\mathbf{G}_{\mathrm{n}}^{\mathrm{T}}\mathbf{C}_{\mathrm{D}}^{-1}\mathbf{G}_{\mathrm{n}}+\mathbf{I}\right)\Delta\mathbf{m}_{\mathrm{n+1}}=\mathbf{C}_{\mathrm{M}}\mathbf{G}_{\mathrm{n}}^{\mathrm{T}}\mathbf{C}_{\mathrm{D}}^{-1}\left(\mathbf{d}_{\mathrm{obs}}-\mathrm{g}(\mathbf{m}_{\mathrm{n}})\right)+\left(\mathbf{m}_{\mathrm{prior}}-\mathbf{m}_{\mathrm{n}}\right). \qquad (3)$$

where $\Delta\mathbf{m}_{n+1} = \mathbf{m}_{n+1} - \mathbf{m}_n$. The resulting, non-symmetric system can be solved efficiently using the quasi-minimum-residual-biconjugate-stable algorithm (QMRCGSTAB) introduced by Chan et al. (1994).

The ERT method tends to show poor sensitivity in the center of 3-D volume away from the electrodes. To provide more uniform image quality, an empirical scheme adapted from Morelli and LaBrecque (1996) was implemented to alter the parameter standard deviations:

$$\sigma'_{mi} = \sigma_{mi} \cdot \{ \mathrm{diag}(\mathbf{G}^{\mathbf{T}}\mathbf{G})_i \}^{-\mathbf{n}}, \quad i = 1, 2, \ldots, M. \qquad (4)$$

where σ_{mi} is the *a priori* standard deviation of i-th model parameter, σ'_{mi} is the model standard deviation after weighting, M is the total number of model parameters, and n is an empirical weighting factor which ranges from 0.10 to 0.30. Optimal values for n were determined empirically to be approximately 0.2.

Figure 4 shows the results of inverting synthetic model data using the new stochastic inversion algorithm. These results are similar to those produced by an older inversion scheme that employs the Occam's approach (Labrecque et al, 1999) to yield a model that smoothly varies across the image domain.

3.2.3 Application to the STVZ Experiment

Empirical relations such as that of Archie (1942) and Waxman and Smits (1968) give a functional relation between resistivity and porosity, fluid salinity, moisture content, and the cation-exchange capacity (CEC) of the various mineral constituents. Thus moisture content can be estimated from resistivity if the other parameters (porosity, CEC etc.) are known. This was not practical for our application in which the available data was the ERT resistivity images coupled with spatially sparse hydrological measurements. The solution was to determine a local, empirical relationship between resistivity and moisture content for the 'background' images generated from data collected before the infiltration began, and a second expression that relates changes in resistivity to changes in moisture content during infiltration. The first of these relations is based on the assumption that the undisturbed system prior to infiltration has reached equilibrium, and that in such a system the moisture content is primarily a function of the grain size distribution. Since the grain size distribution will control the CEC, and to some extent the porosity, all of the important parameters should be strongly correlated. We used a relationship of the form

$$\rho_t = a \cdot \theta^b \qquad (5)$$

where ρ_t is the resistivity of partially saturated sediments, θ is moisture content; and a and b are empirical constants that were determined by comparing resistivity values to neutron derived moisture contents. We found good comparisons between the ERT estimated moisture contents and those derived from the neutron data using $a = .021$ and $b = -3.2$. These constants are very different from those normally employed in formulas similar to that of Archie (1942) since they reflect not only the relationship between saturation and resistivity, but also the correlation between grain size and residual water content in the unsaturated sediments.

The changes in resistivity caused by increased moisture content during infiltration can also follow the power law relation given by Equation (5), but the constants, a and b, are more typical of those employed in Archie's law (Archie, 1942). Using laboratory measurements of resistivity versus saturation that were made on 12 core samples collected at the site, we chose a value of $b = -1.5$, the geometric mean of the 12 samples. These laboratory measurements were made on the wetting/saturation phase using water from the same source as employed in the field infiltration experiment. The coefficient, a, varied substantially from sample to sample (not shown). To determine this value, the background moisture

content was determined, and then the value of *a* in the post-infiltration formula was allowed to vary from cell to cell such that the pre- and post-infiltration equations matched for the background data set.

Figure 2 shows the plan view of the ERT electrodes at the STVZ site, and Figure 5 shows the image of the estimated moisture content for data prior to infiltration in February of 1999. Regions of high water content are shown as blue, and those of low water content are transparent. Some of the prominent features of this image include the strongly resistive, low-water content zone at the top of the image corresponding to the dry sand and gravel layers, and zones corresponding to the clay layers between 3 and 6 m in depth. Note that the infiltration pad is centered on the block. The plot extends from the surface to a depth of 13 m.

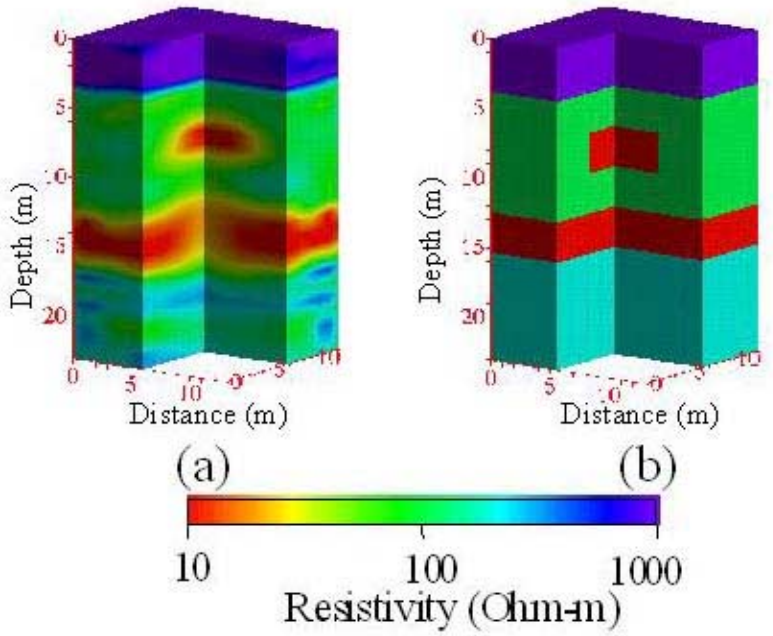

Figure 4: ERT inversion results from a synthetic model (a) compared with the true model (b).

In Figure 6 differences between the post- and pre-infiltration images have been plotted for four different time periods. The results are plotted in a format that makes any change less than +3 percent volumetric moisture content invisible, and all changes greater than that are blue to purple. Notice that early on in the infiltration the changes are confined to the upper few meters, although non-symmetric, or heterogeneous flow is apparent early on. Also notice that as time increases, the horizontal extent of the plume also increases as the clay layers inhibit downward flow. However, and maybe more importantly, a preferential flow path appears in the two latter images where a high moisture content zone appears from the bottom of the plume to depth. This is most likely preferential flow occurring down one of the ERT boreholes. These boreholes were backfilled with surface sand rather bentonite to avoid electrical shorting between electrodes, and therefore consist of coarse, permeable sand along their entire length. The results are important in that they indicate that this type of man-made disturbance can serve as flow and transport pathways, even though they are in the unsaturated zone.

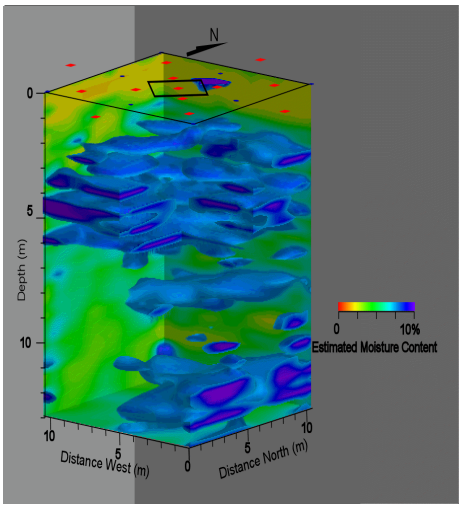

Figure 5: 3D Estimated pre-infiltration moisture content for the STVZ from ERT.

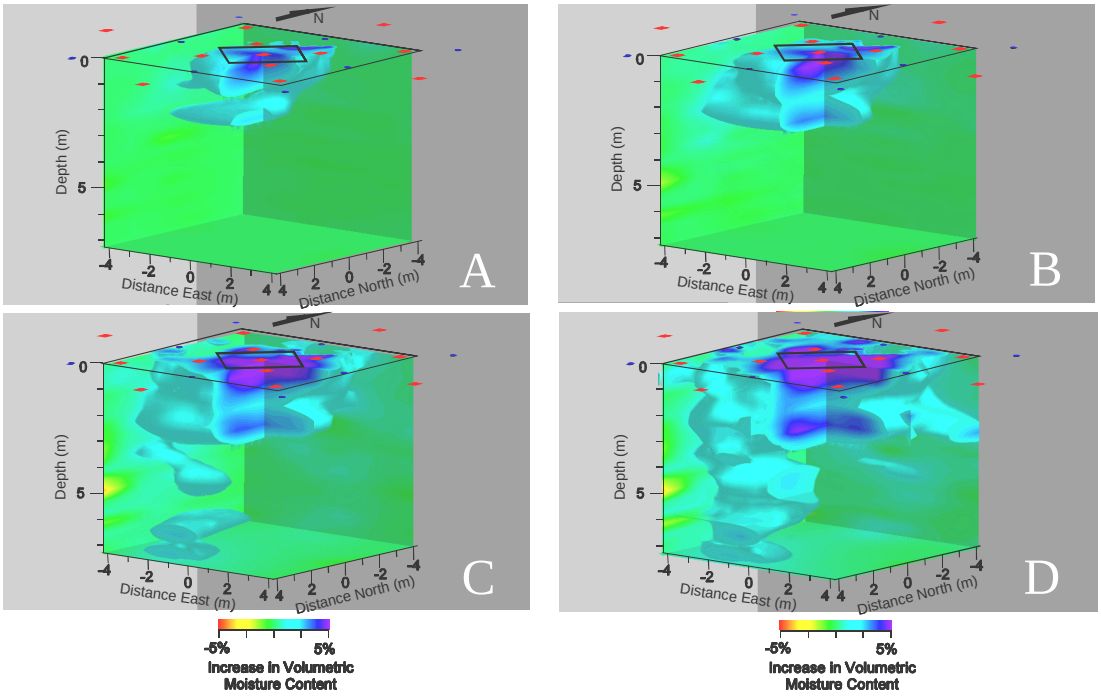

Figure 6: Moisture content estimated from ERT data at four times: March 20, 1999 after 9 days of infiltration (A), April 13 after 33 days of infiltration (B), June 1, 1999 after 82 days of infiltration (C) and July 22, after 133 days of infiltration (D).

3.3 Cross Borehole Ground Penetrating Radar (XBGPR) Imaging of the Sandia-Tech Vadose Zone Site Experiment

Cross borehole ground-penetrating radar (XBGPR) data were collected between the PVC access tubes along the SW to the NE stretching across the infiltrometer (see Figure 2). The purposes for including this geophysical method were; 1) to provide a check on the ERT results; 2) to provide high resolution measurements of the moisture content field than that from ERT for examining smaller scale features; and 3) to help assess the ability of the two methods for recovering images of moisture content. Higher resolution in the XBGPR measurements was the result of closer borehole spacing and smaller

source and receiver sampling intervals.

3.3.1 Background

The GPR method employs an electrical dipole source that operates at frequencies ranging between 10MHZ and 1GHz. At these frequencies, the electromagnetic (EM) energy propagates as a wave, albeit an attenuating wave, and thus techniques developed for seismic travel-time imaging can be applied to GPR data to obtain first arrival times to produce high- resolution images of the subsurface. Because the EM wave velocities at these frequencies are significantly slowed by water within geologic formations, GPR measurements provide the means to measure moisture content fields between the transmitter and receiver.

3.3.2 Application to the STVZ Experiment

AT the STVZ, XBGPR measurements were obtained along the NE-SW profile. Therefore a 2-D profile of volumetric moisture content was provided. A Sensors and Software Pulse-EKKO 100 system was employed for data acquisition using a center frequency of 100 MHz and a down hole source and receiver sampling interval of 0.25m. Data were collected between the five wells yielding four individual cross-well data sets. First arrival times were first "picked" using software provided by Sensors and Software, then they were inverted using a scheme developed by Aldridge and Oldenberg (1993) to produce a 2D image of EM wave velocity, v. The acquisition angle between the source and receiver never exceeded 45°. For angles greater than this experiments showed that the wires that had been placed in the ground for the ERT and hydrologic sensors created interference that led to a distortion in the measured wave field, and thus incorrect first arrivals. For angles less than this the first arrival time was unaffected.

Velocity was converted to apparent dielectric constant (ε_a), defined as $\varepsilon/\varepsilon_0$ where ε_0 is the permitivity of free space with a value 8.85×10^{-12} F/m, using the expression

$$\varepsilon_a \cong (c/v)^2 \tag{6}$$

where c is the speed of light (0.3 m/ns). The final processing step was to convert the image of ε_a to that of volumetric moisture content using an empirical relationship between dielectric constant and moisture content;

$$\theta=(0.0136*\varepsilon-0.033). \tag{7}$$

This expression was derived from a calibration procedure for time-domain reflectometry (TDR) probes which was conducted in the laboratory on hand samples collected at the site, thus providing a linear relationship between ε_a and volumetric moisture content. Like XBGPR, the TDR provides moisture contents indirectly through measurements of an EM wave velocity, which is then converted to a dielectric. The dielectric is then related to moisture content through a calibration procedure. Figure 7 shows an example of the TDR data employed in this calibration along with moisture contents that would be predicted if commonly used expression know as Topp's equation (Topp et al., 1980) were to be employed. Most likely the disparity between these two estimates of moisture content is due to the presence of magnetic minerals in the soil which is not accounted for in equation (6) or in Topp's equation.

In Figure 8 XBGPR moisture content images are plotted along the profile for data collected prior to the beginning of infiltration, and 8, 35 and 135 days after infiltration began. For comparison, calibrated neutron measurements are included on these images, and appear as vertical bars extending downward from positions at -5.5m, -2.5m, 0m, 2.25m, and 5.25m along the surface. Note that there appears to be quite a bit of heterogeneity present in the images, and that the XBGPR and neutron data sets qualitatively compare well. However, there are differences, primarily in that 1) the XBGPR image is a 'smoother' version of the neutron logs, and 2) in the XBGPR does not recover the high moisture zone in the center well near the surface. Alumbaugh et al. (2000) state that the former is due to limitations in the

imaging configuration and the processing that is applied to the data, while the latter is due to limitations of the method in imaging near-surface features. Alumbaugh et al. (2000) also determine from multiple data sets collected prior to the infiltration that the RMS accuracy error between the neutron and the XBGPR images at the borehole locations is 2.3 percent volumetric moisture content, while the repeatability or precision error is 0.5 percent volumetric moisture content.

Comparisons between the preinfiltration moisture content image (Figure 8a) and the three post infiltration images (Figures 8b through 8d) shows that the water is infiltrating into the subsurface around the center well. A more detailed view of the bulb can be obtained by taking the difference between the post and pre infiltration images as shown for the four different post infiltration times in Figure 9. Notice that the images show the wetting front to be asymmetric with more of the water heading to the SW compared to the NE. This agrees somewhat with the differenced neutron logs in Figure 10 that show large changes in the inner SW well, and smaller changes in the inner NE well. Also it appears to agree qualitatively with the 3D ERT images in Figure 6. Finally, notice that there appears to be quite a bit of heterogeneity within the imaged flow field. Although not all of the imaged heterogeneity represent moisture content changes that fall above the stated accuracy and repeatability error levels, much of it does which indicates that this heterogeneity is likely to be real.

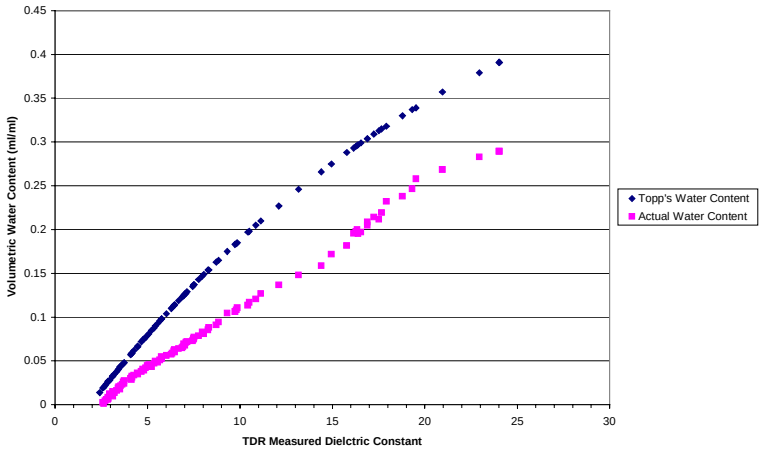

Figure 7: TDR measured apparent dielectric constant versus actual moisture content and that estimated using Topp's equation (Topp et al., 1980) for a soil sample collected at the Socorro infiltration site.

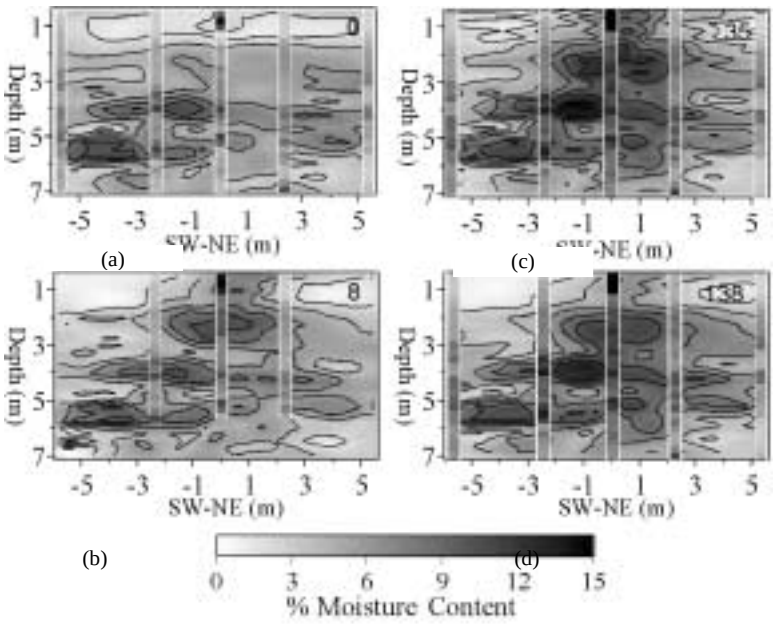

Figure 8: Moisture content images derived from the XBGPR measurements before and after infiltration. The number in the upper right corner refers to the number of days after infiltration began that the data were collected. The vertical stripes of color correspond to neutron moisture measurements made at those locations.

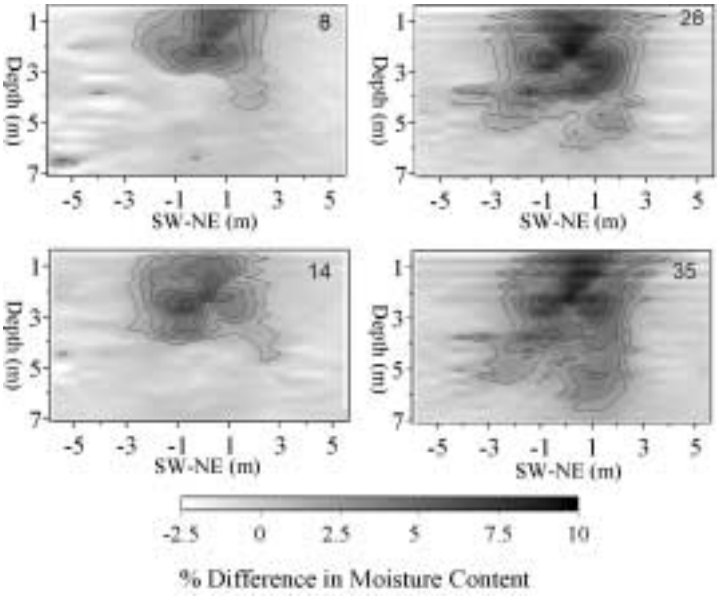

Figure 9: Images of differences in moisture content between pre- and post-injection images. The number in the upper right corner refers to the number of days after infiltration began that the XBGPR data were collected. The contours are at intervals of 1-percent volumetric moisture content.

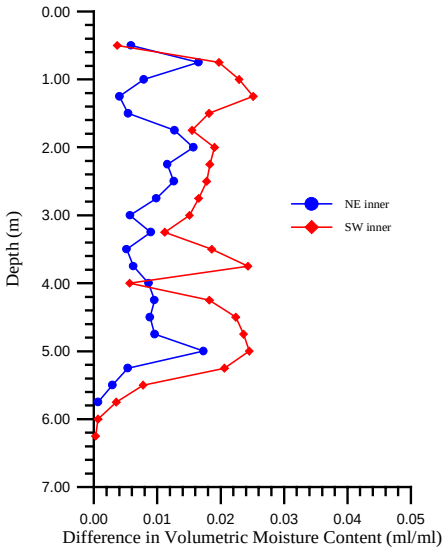

Figure 10: Moisture content changes between neutron data collected before infiltration and at day 35.

3.4 Vadose Zone Inverse Modeling

3.4.1 Background

In general, solutions to inverse problems of flow through porous media are non-unique. It is a well-known fact that it is impossible to correctly identify the spatial distribution of hydraulic conductivity in an aquifer under steady-state flow conditions unless all the hydraulic heads are known and boundary fluxes are specified. For cases with given scattered hydraulic head and hydraulic conductivity measurements, a rational approach would rely on the conditional stochastic concept. In other words, one should attempt to obtain the natural log of saturated hydraulic conductivity ($\ln Ks$), the natural log of pore-size distribution coefficient ($\ln \alpha$), soil-water pressure head (ψ), and effective saturation (Θ) fields that not only preserve their observed values at all sample locations, but also satisfy their underlying statistical properties (i.e., mean and covariance). Furthermore, the estimated $\ln Ks$, α, and ψ fields should satisfy the governing flow equation and effective saturation expression. In the conditional probability concept, these estimated fields are conditional realizations of the ensemble and many possible realizations of such conditional fields exist. One method of dealing with such a non-uniqueness problem is to derive the expected values of all possible conditional realizations instead of each individual conditional realization. This is the goal of the hydrological inverse algorithm that resulted from this research.

3.4.2 Inverse Modeling Theory

An inverse model to estimate hydraulic properties of three-dimensional, heterogeneous vadose zone using moisture content and pressure measurements has been developed. The model assumes that movement of water in partially saturated porous media under isothermal conditions, neglecting the gas phase, is described by

$$[\beta S_s + C(\psi)]\frac{\partial \psi}{\partial t} = \nabla \cdot [K(\psi)\nabla(\psi + z)] \tag{8}$$

where ψ is pressure head, which is positive when soil is fully saturated and is negative when the soil is

partially saturated, and z is the positive upward vertical coordinate. The term S_s represents specific storage and β is a transitioning parameter that is unity when ψ is greater than or equal to zero, and zero when ψ is negative. To describe the saturation-pressure head relationship of unsaturated media, Mualem's model is used:

$$S = \frac{\theta - \theta_r}{\theta_s - \theta_r} = \left(1 + \left|\alpha\psi\right|^n\right)^{-m} \tag{9}$$

where S is degree of saturation, θ is volumetric moisture content, θ_s is saturated moisture content, θ_r is moisture content at residual saturation and α, n, and m are fitting parameters with $m = 1 - 1/n$. This relationship leads to the following expression for the moisture capacity term, $C(\psi)$,

$$C(\psi) = \alpha(n-1)(\theta_s - \theta_r)S^{1/m}\left(1 - S^{1/m}\right)^m, \tag{10}$$

and the unsaturated hydraulic conductivity,

$$K(\psi) = K_s\sqrt{S}\left(1 - \left(1 - S^{1/m}\right)^m\right)^2, \tag{11}$$

[*van Genuchten*, 1980] where K_s is saturated hydraulic conductivity. Based on these models, the unsaturated hydraulic properties of a porous medium can be characterized if values of the parameters K_s, α, and n are specified, assuming saturated and residual moisture contents are known.

In the inverse model, K_s, α, and n are treated as stochastic processes in order to represent the heterogeneity of geological formations under unsaturated conditions. We assume these stochastic processes are characterized by exponential covariance functions with the parameters of mean, variance, and correlation scale assumed known. The saturated and residual moisture contents are treated as deterministic constants due to the typically small variability of these parameters [*Russo and Bouton*, 1992]. Incorporation of spatial variability in θ_s and θ_r into the model, however, is straightforward should it be important for a specific application.

To estimate the parameters, K_s, α, and n, our inverse approach relies on measurements of the parameters, pressure head, and moisture content and their statistical moments (namely, mean, covariances and cross-covariances). The covariances and cross-covariances of pressure head, and moisture content are calculated using a first-order analysis described as below. First, state variables are expanded in a Taylor series around the means in the general form

$$u = \langle u \rangle + \sum_i \chi_i \left.\frac{\partial u}{\partial \mathrm{X}_i}\right|_{\langle \mathrm{X}_i \rangle, \langle u \rangle} \tag{12}$$

where u is the state variable ψ or θ, the summation is of the stochastic parameters, and terms of second and higher order are neglected. In this expression $\chi_i = \mathrm{X}_i - \langle \mathrm{X}_i \rangle$ represents the zero mean perturbation in a log transformed hydraulic parameter such as $f = \ln(K_s) - \langle \ln(K_s) \rangle$, $a = \ln(\alpha) - \langle \ln(\alpha) \rangle$, or $\nu = \ln(n) - \langle \ln(n) \rangle$ and the angle brackets denote the expected value. Perturbations in the state variables, $\upsilon = u - \langle u \rangle$, also have a mean of zero. Sensitivity derivatives in (12) are computed by the adjoint state method. Details of this derivation can be found in Hughson and Yeh [2000].

Notice that one must derive the mean pressure head, $\langle \psi \rangle$, first in order to evaluate the

sensitivities discussed above. To do so, the mean equation is assumed to be the same as the Richards equation (8), and $K(\psi)$ and $C(\psi)$ are assumed to be described by (9) through (11) with parameter values set to their mean values [*Yeh*, 1998]. Thus, a zero order mean pressure head can be obtained by solving

$$\left[\beta S_s + C\left(\langle\psi\rangle\right)\right]\frac{\partial\langle\psi\rangle}{\partial t} = \nabla\cdot\left[K\left(\langle\psi\rangle\right)\nabla\left(\langle\psi\rangle + z\right)\right] \tag{13}$$

In this study, a finite element program (MMOC3) developed by *Srivastava and Yeh* [1992] was modified to obtain the solutions to (8) and (13).

Once the mean pressure head is obtained, the above sensitivity equations can be used to calculate covariances and cross-covariances needed in our inverse approach. The expressions for the cross-covariances of head and moisture content with hydraulic properties can be derived by first discretizing the flow domain into j blocks or elements, multiplying (12) by perturbations in f, a, and v, and then taking the expectation to yield

$$\mathbf{R}_{\upsilon\chi} = \mathbf{R}_{\chi\chi}\mathbf{J}_{\upsilon\chi}. \tag{14}$$

In this expression $\mathbf{R}_{\upsilon\chi}$ is notation for the cross-covariance matrix $\langle\upsilon\chi\rangle$ of the zero mean perturbations in parameters and state. The $j\times j$ matrices $\mathbf{R}_{\chi\chi}$ for the covariance functions of the log transformed perturbations of the hydraulic properties K_s, α, and n are assumed known. Cross-covariance matrices $\mathbf{R}_{\upsilon\chi}$ have dimensions $j\times n_d$ where n_d is the notation for the number of head or moisture content data. The Jacobian, or sensitivity matrices, $\mathbf{J}_{\upsilon\chi}$, also are $j\times n_d$. In the formulation of (14) we have assumed that the hydraulic properties are independent. Note that our assumption of independence represents the worst case, implying that information about one parameter tells us nothing about others.

Covariances of the perturbations in pressure head, $h = \psi - \langle\psi\rangle$, and moisture content, $s = \theta - \langle\theta\rangle$, are derived by multiplying (5) by the perturbations, taking the expectation, and substituting (14) to yield

$$\mathbf{R}_{\upsilon w} = \sum_{\chi}\mathbf{J}_{\upsilon\chi}^{T}\mathbf{R}_{\chi\chi}\mathbf{J}_{w\chi} \tag{15}$$

where T indicates transpose. Covariances are obtained when υ and w are perturbations of the same state variable, and cross-covariances are obtained when υ is h and w is s. Covariances of the secondary information in (15) are $n_d\times n_d$ matrices. Note that the cross-covariance matrix computed in (15) need not be symmetric. Second-order approximations of these covariances can be obtained by the method developed by *Liedl* [1994].

Using these covariances, a first-order estimate of the perturbations in the hydraulic properties that incorporates secondary information from the pressure head and moisture content variables, can be obtained by solving the cokriging equations

$$\begin{bmatrix} \mathbf{C}_{\chi\chi} & \mathbf{C}_{s\chi} & \mathbf{C}_{h\chi} \\ \mathbf{C}_{s\chi}^{T} & \mathbf{R}_{ss} & \mathbf{R}_{hs} \\ \mathbf{C}_{h\chi}^{T} & \mathbf{R}_{hs}^{T} & \mathbf{R}_{hh} \end{bmatrix}\begin{bmatrix} \lambda_{\chi} \\ \lambda_{s} \\ \lambda_{h} \end{bmatrix} = \begin{bmatrix} \mathbf{R}_{\chi\chi}^{T} \\ \mathbf{R}_{s\chi}^{T} \\ \mathbf{R}_{h\chi}^{T} \end{bmatrix} \tag{16}$$

In this matrix formulation the symbol χ indicates the primary variable being estimated and $\mathbf{C}_{\chi\chi}$, $\mathbf{C}_{s\chi}$, and $\mathbf{C}_{h\chi}$ represent covariances and cross-covariances of the data which are subsets of covariance and

cross-covariance matrices obtained from (14) and (15). Note that the top element on the right hand side of (9), $\mathbf{R}_{\chi\chi}^{\mathbf{T}}$, is the specified covariance of the parameter field. It is a j by number of parameter data subset of $\mathbf{R}_{\chi\chi}$ that does not change during iteration. The $n_d \times j$ matrices λ_χ, λ_s, and λ_h are the cokriging weights applied to data of the primary variable and the secondary information on moisture content and pressure. On the right hand side of (16) are the covariances and cross-covariances of the data with the primary variable to be estimated. These transposed covariance matrices have rows equal to the number of data and j columns. The cokriging weights are also matrices of the same dimension. Once the weights are evaluated, linear estimates of the hydraulic properties are

$$\hat{\chi} = \lambda_\chi^T \chi_d + \lambda_s^T s_d + \lambda_h^T h_d \tag{17}$$

where $\hat{\chi}$ is a $j \times 1$ vector of the estimated perturbation in a hydraulic property and χ_d, s_d, and h_d are data of perturbations in the hydraulic property, moisture content, and pressure head.

Estimates of soil hydrological properties obtained from (17) match measurements that are made on samples, and also incorporate the information from pressure and moisture content data. However, cokriging is a linear estimator while the physical relationships between the parameters and system states, described by (8) through (11) are highly nonlinear. As a consequence, the pressure and/or moisture content information is not fully utilized by cokriging, and thus the estimated parameter fields are thus not as detailed as they could be. In order to fully incorporate the nonlinearity of the problem and utilize information about hydrological properties from all of the data, we have employed an iterative technique similar to *Yeh et al.* [1996], *Zhang and Yeh* [1997] and *Hanna and Yeh* [1998]. This iterative method, referred to as a successive linear estimator, or SLE, will be briefly summarized here.

First the cokriging weights from (16) are used to compute the residual parameter covariances as

$$\mathbf{R}_{\chi\chi}^{(1)} = \mathbf{R}_{\chi\chi}^{(0)} - \breve{\mathbf{R}}_{\chi\chi}^{(0)} \lambda_\chi - \mathbf{R}_{h\chi}^{(0)} \lambda_h - \mathbf{R}_{s\chi}^{(0)} \lambda_s , \tag{18}$$

where $\breve{\mathbf{R}}_{\chi\chi}^{(0)}$ is a $j \times n_d$ subset of $\mathbf{R}_{\chi\chi}^{(1)}$ and χ represents one of the parameters f, a, or ν. The superscript in parentheses is the iteration index. Next the data-conditioned parameter fields estimated in (17) are used in the flow model to solve for conditional pressure and moisture content. These parameter fields and the resulting pressure and moisture content fields are then used to solve the adjoint state and sensitivities equations. Multiplying these conditioned sensitivities by the residual covariances calculated in (18), as in (14) and (15), gives updated covariances and cross-covariances. Residual cokriging weights are then calculated from

$$\begin{bmatrix} \mathbf{R}_{hh}^{(r)} & \mathbf{R}_{hs}^{(r)} \\ \mathbf{R}_{hs}^{(r)} & \mathbf{R}_{ss}^{(r)} \end{bmatrix} \begin{bmatrix} \lambda_h^{(r)} \\ \lambda_s^{(r)} \end{bmatrix} = \begin{bmatrix} \left(\mathbf{R}_{h\chi}^{(r)}\right)^T \\ \left(\mathbf{R}_{s\chi}^{(r)}\right)^T \end{bmatrix}, \tag{19}$$

and the successive linear estimate of the parameter perturbations is given by

$$\hat{\chi}^{(r+1)} = \hat{\chi}^{(r)} + \lambda_h^{(r)} \left(\psi_d - \psi^{(r)}\right) + \lambda_s^{(r)} \left(\theta_d - \theta^{(r)}\right), \tag{20}$$

where $\psi^{(r)}$ and $\theta^{(r)}$ are pressure and moisture content at the data locations calculated from the flow model using parameter estimates at iteration r. Pressure and moisture content data are the vectors ψ_d and θ_d, and $\hat{\chi}^{(r)}$ represents the parameter estimate at iteration r. As the residual cokriging weights are computed, they are used to update the residual parameter covariances for the next iteration

$$\mathbf{R}_{\chi\chi}^{(r+1)} = \mathbf{R}_{\chi\chi}^{(r)} - \mathbf{R}_{h\chi}^{(r)} \lambda_h - \mathbf{R}_{s\chi}^{(r)} \lambda_s \ . \tag{21}$$

Iteration continues until variance of the estimated parameter field changes by less than some specified small value between iterations. As the iteration progresses, the solution of (19) and (20) is complicated by the fact that the data covariance matrix on the left-hand side of (19) may become nearly singular. This problem is mitigated by adding a stabilizer term, a multiple of the largest diagonal value, to the diagonal of the matrix in (19). A multiplication factor between 1 and 4 typically results in a well-conditioned residual covariance matrix. Notice that the dimension of the matrix in (19) is on the order of the total number of data. Small matrix dimensions improve the computational efficiency of the SLE method as compared to other parameter estimation techniques, such as the Gauss-Newton search approach.

3.4.3 Application to the STVZ Experiment

The aforementioned hydrological inverse model was applied to the data collected at the experiment site. Tensiometer and neutron data collected at day 138 after infiltration were used as the secondary information in a steady-state hydrological inversion to estimate the K_s, α, and n fields. Hydraulic parameter values that were measured on samples collected from the northeast continuous core hole (Figure 1) were used as the primary information in the estimation process. Since it is difficult to estimate horizontal correlation scales at the field site, different correlation scales were tested (e.g., horizontal correlation lengths of 10 m and 40 m and 1.5 m for vertical correlation length). Based on reconstructed geological stratigraphy, we concluded that the longer horizontal correlation length (40 m) produced somewhat more realistic, stratified K_s, α, and n fields, at the experimental site. From our previous numerical experiments, pressure head measurements were found to be useful for estimating K_s and moisture content measurements were effective for estimating α, and n fields.

Figure 11 shows the estimate of the K_s based on 43 tensiometer measurements, while Figures 12 and 13 show the α, and n fields estimated from 312 neutron measurements, respectively. These figures demonstrate that the inverse model offers promise as a characterization tool. The estimated fields closely resemble the geological stratigraphy reconstructed based on the borehole information. However, their accuracy in representing the true hydraulic parameter fields for the field site need to be verified. Two methods for doing so would be extensive sampling, and numerical simulation to determine if the resulting model can reproduce the field experiments under different initial and boundary conditions.

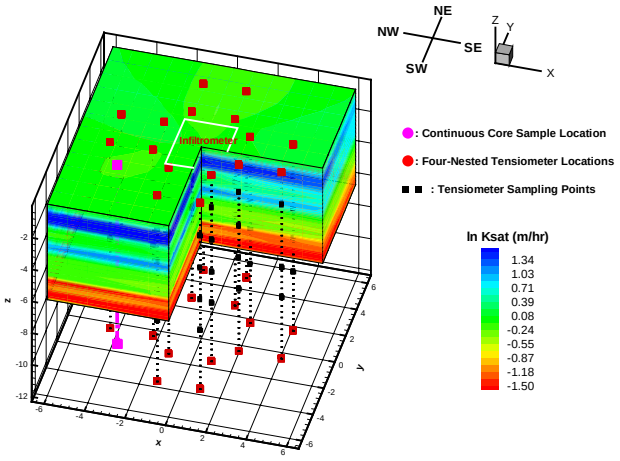

Figure 11: Geostatistical inversion results showing the 3-D distribution of saturated hydraulic conductivity estimates at the STVZ. This data was obtained using point measurements of matric potential from 43 tensiometers with correlation length scales of X = Y = 40m and Z = 1.5m.

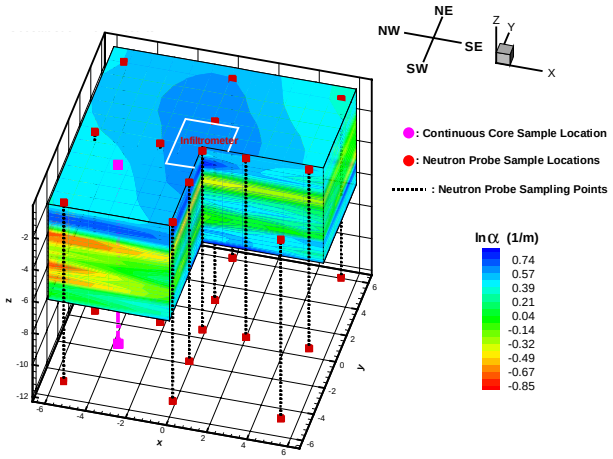

Figure 12: Geostatistical inversion results showing the 3-D distribution of the α estimates at the STVZ. This data was obtained using point measurements of moisture content from 312 neutron data with correlation length scales of X = Y = 40m and Z = 1.5m.

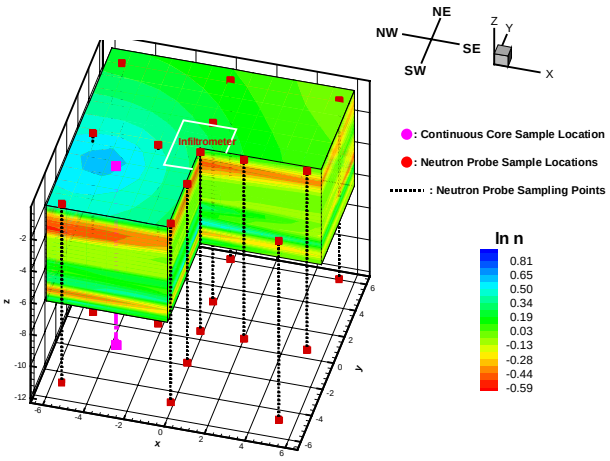

Figure 13: Geostatistical inversion results showing the 3-D distribution of the *n* estimates at the STVZ. This data was obtained using point measurements of moisture content from 312 neutron data with correlation length scales of X = Y = 40m and Z = 1.5m.

3.5 Conclusions

A controlled infiltration experiment has been performed to produce unsaturated flow conditions, and mimic contaminant flow and transport processes that may be occurring at many DOE sites. Two geophysical imaging methods (ERT and XBGPR) that have been extended show great promise in being able to image and monitor changes in moisture content that result in such cases. A hybrid geophysical/hydrological inverse method has also been developed for ascertaining hydrologic properties of the subsurface. This method has been tested on both synthetic results as well as the data collected at the STVZ site, and it shows great promise as a subsurface hydrologic characterization tool.

4 Relevance, Impact and Technology Transfer:

a. How does this new scientific knowledge focus on critical DOE environmental management problems?

The new scientific knowledge gained from this research project impacts assessment for a wide range of monitoring applications but is particularly important for vadose zone monitoring. This knowledge provides a method to more accurately assess hydrologic parameters at a given site.

b. How will the new scientific knowledge that is generated by this project improve technologies and cleanup approaches to significantly reduce future costs, schedules, and risks and meet DOE compliance requirements?

Employing the methodology developed in this project (field experiment and data processing) in materials characteristic of a contaminated site would provide measures of otherwise unavailable 3-d distributions of unsaturated hydrologic properties. Incorporation of these properties into predictive models would then provide more accurate estimates of fluid transport velocities allowing for a more accurate risk assessment. Also, employing the geophysical methods, along with the data processing techniques developed for this project, would provide quantitative measures of hydrologic conditions necessary for successful long-term monitoring strategies.

c. To what extent does the new scientific knowledge bridge the gap between broad fundamental research that has wide-ranging applications and the timeliness to meet needs-driven applied technology development?

This research bridges the gap through the development of additional tools which are readily useable for site specific applications. These tools provide fundamental insight into vadose zone fluid flow processes and provide 3-D distributions of estimated unsaturated hydrologic properties. This new scientific technology can be applied to any site with a vadose zone, not just at DOE sites. Additionally, this research has already had significant impacts on field methodologies. For example, results from the HHGIT field and theoretical studies have prompted substantial changes in the way that ERT data is collected and processed.

d. What is the project's impact on individuals, laboratories, departments, and institutions? Will results be used? If so, how will they be used, by whom, and when?

The impact is mostly on the individual and department level. These results will hopefully be used for the calibrating of others predictive models in the near future.

e. Are larger scale trials warranted? What difference has the project made? Now that the project is complete, what new capacity, equipment, or expertise has been developed?

Larger field scale trials are warranted at contaminated sites such as Hanford.

f. How have the scientific capabilities of collaborating scientists been improved?

New inversion algorithms have been created which allow for scientists involved within the project to more accurately and fully interpret the geophysical and hydrologic data. In addition, the scientists now better understand the limitations and advantages of the various instruments that were employed.

g. How has this research advanced our understanding in the area?

This research has resulted in an improved understanding of the relationships between geophysical images of the subsurface, hydrological measurements, hydrological conditions, and hydrological parameters.

h. What additional scientific or other hurdles must be overcome before the results of this project can be successfully applied to DOE Environmental Management problems?

There is a need to move incrementally toward full-scale deployment of these technologies. This implies that a close collaboration between technology developers and end-users that may require pilot studies at contaminated sites is required. In an era of increasingly tight budgets, end users are often reluctant or unable to fund initial deployments of these technologies despite their long-term benefits. There is a need to create an environment with both the funding and management incentives to create collaborations between users and developers.

i. Have any other government agencies or private enterprises expressed interest in the project?

Yes, Hanford, INEEL, Savannah River.

5 Project Productivity:

Did the project accomplish all of the proposed goals? If not, why not? Was the project on schedule? Was the work plan revised? If so, describe revision.

The project encountered delays during the first funding year due to the inability to locate a suitable field site. Plans of having the field site at Sandia National Laboratories (SNL) were thwarted by a combination of unforeseen circumstances. Although several locations were suitable for the field site at SNL, only one site was available for the entire period of the project. Late in the process of obtaining the appropriate approvals and permits, we learned that the Environmental Remediation group was planning to excavate a nearby landfill. Because the exact contents of the landfill were unknown, there was a good chance that we might not have continuous access to the site. Hence, we decided to locate the site at New Mexico Technical Institute in Socorro, NM. In addition, Dr Jim Yeh from the University of Arizona, a Co-PI on the project experienced a set back on the theoretical development of the HHGIT due to the untimely departure of a Post Doctoral researcher who accepted a permanent position elsewhere.

Despite these setbacks, many of the project goals were accomplished due to a No Cost One-Year Extension granted at the end of FY 1999. One area of technical difficulty we encountered involved development of the inverse approach where the joint inversion of the geophysical and hydrological data was to provide 3-D distributions of the unsaturated hydraulic property parameters. We found that the simultaneous inversion is computationally beyond what could be done in a three-year period. Difficulties in obtaining the solution for unsaturated flow simulation often prolong the computational time for forward simulation and prohibit the inversion of the full-scale field experiment. In addition, the inversion is highly sensitive to the error in the moisture content estimates. An alternative iterative approach was developed where the hydrological inversion method described above is implemented on point measurements of the pressure field and moisture content data. Then, to improve on the results, the 3-D moisture content field from the ERT is used as update to provide higher resolution and more certain estimates of the unsaturated hydrologic properties.

6 Personnel Supported:

Dr. David L. Alumbaugh: Sandia National Laboratories, Albuquerque, NM

Dr. Alumbaugh's student collaborator

Lee Paprocki: Master student at New Mexico Technical Institute of Mining and Technology.

Dr. Robert J. Glass: Sandia National Laboratories, Albuquerque, NM

Dr. Glass' student collaborator

Christine Smith: Student Intern at Sandia National Laboratories; Master student at New Mexico Technical Institute of Mining and Technology.

Dr. Christopher Rautman: Sandia National Laboratories, Albuquerque, NM

James Brainard: Student Intern at Sandia National Laboratories, Albuquerque, NM - MS thesis at University of New Mexico; Limited Term Employee Sandia National Laboratories.

Dr. T. C. Jim Yeh: Department of Hydrology and Water Resources, University of Arizona.

Dr. Yeh's student collaborators:

Debra Hughson: Post Doctoral Student, University of Arizona

J.A.Vargas-Guzman: Post Doctoral Student, University of Arizona

Hsin-Chia Chao: Post Doctoral Student, University of Arizona

Bailing Li, Ph.D. Student, University of Arizona

Shuyung Liu: Ph.D. Student, University of Arizona

Martha Whitaker, Ph.D. Student, University of Arizona

Chunjun Li, Ph.D. Student, University of Arizona

Derek Blazer, Master Student, University of Arizona

Ryan Gardiner, Master Student, University of Arizona

Dr. Douglass LaBrecque – University of Arizona; Steam Tech Environmental Services; and MultiPhase Technologies

DR. LaBrecque's student collaborators

Emily Sullivan, MS. University of Arizona

Gail Heath, MS. University of Arizona

Xiajing, Yang, Ph.D. University of Arizona

7 Publications:

Peer Reviewed Journals

Alumbaugh, D. L., Paprocki, L., Brainard, J., Glass, R.J., and Rautman, C., 2000, Estimating in-situ moisture contents using cross-borehole ground penetrating radar; a study of accuracy, repeatability and resolution, to be submitted to Water Resources Research.

Hughson, D.L. and T.-C. J. Yeh, A geostatistically based inverse model for three-dimensional variably saturated flow, Stochastic Hydrology and Hydraulics, 12, 285-298, 1998.

Hughson, D.L. and T.-C. J. Yeh, An inverse model for three-dimensional variably saturated flow, Water Resources Research,36(4), 2000.

Li, B. and T.-C. J. Yeh, Cokriging estimation of the conductivity field under variably saturated flow conditions, Water Resour. Res., 35(12), 3663-3674, 1999.

LaBrecque, D., and Yang, X, 2000, Difference inversion of ERT data - a fast inversion method for 3-D in-situ monitoring, submitted to Journal of Environmental and Engineering Geophysics.

LaBrecque, D. J., Yang, X., Alumbaugh, D. L., and Paprocki, L., 2000. Three-dimensional monitoring of vadose zone infiltration using ERT and cross-borehole ground penetrating radar, in preparation.

Vargas-Guzman, J. A., and T.-C. J. Yeh, Sequential kriging and cokriging: two powerful geostatistical approaches, Stochastic Environmental Research and Risk Assessment, 13(6), 416-435, 1999.

Yang, X., and LaBrecque, D.J., 2000, Stochastic inversion of 3-D ERT data, to be submitted to *Geophysics*.

Yeh, T.-C. J. and S. Liu, Hydraulic tomography: development of a new aquifer test method, Water Resources Research, 2095-2105, 36(8), 2000.

Liu, S., T. -C. J. Yeh and R. Gardiner, Effectiveness of Hydraulic Tomography: Numerical and Sandbox Experiments, Water Resources Research, accepted, 2000

Conference Papers:

Alumbaugh, D., and Paprocki, L., Monitoring infiltration within the vadose zone using cross-borehole ground penetrating radar; Proceedings of the Symposium on the Application of Geophysics for Environmental and Engineering, Problems Proceeding of the SAGEEP, Arlington VA., pp. 273-281, Feb. 2000.

Brainard, J. R., Alumbaugh, D., Paprocki, L., Glass, R., Baker, K., Labrecque, D., Yang, X., Yeh., T-C J., Rautman, C., Evaluation of Geophysical and Hydrologic Measurements of an Induced Saturation Field within Heterogeneous Deposits, Abstracts from the American Geophysical Union Annual Fall Meeting, San Francisco, CA, 1999.

Brainard, J. R., Alumbaugh, D., Paprocki, L., Glass, R., Baker, K., Labrecque, D., Yang, X., Yeh., T-C J., Rautman, C., A Hybrid Hydrologic – Geophysical Inverse Technique for the assessment and monitoring of leachates in the vadose zone, Abstracts from the American Geophysical Union Annual Fall Meeting, San Francisco, CA, 1999.

LaBrecque, D. J., Yang, X., Alumbaugh, D. L., and Paprocki, L., Three-dimensional monitoring of vadose zone infiltration using ERT and cross-borehole ground penetrating radar: proceedings of Second International Symposium on Three-Dimensional Electromagnetics, Salt Lake City, Utah, 329-332 1999.

Paprocki, L. and Alumbaugh, D., An investigation of cross-borehole ground penetrating radar measurements for characterizing the 2D moisture content distribution in the vadose zone; Proceedings of the Symposium on the Application of Geophysics for Environmental and Engineering Problems Proceeding of the SAGEEP, Oakland CA pp. 583-592 March 1999.

Yang, X., and LaBrecque, D., Three-dimensional complex resistivity tomography, Proceeding of the Symposium on the Application of Geophysics to Environmental and Engineering problems Proceeding of the SAGEEP, Arlington, VA, Feb. 20-24, 2000.

Yang, X., and LaBrecque, D., Estimation of 3-d moisture content using ERT data at the Socorro infiltration site, Proceeding of the SAGEEP, Arlington, VA, Feb. 20-24, 2000.

Yang, X. and LaBrecque, D, Comparison between stochastic and Occam's inversion of 3-D ERT data, Proceeding of the SAGEEP, Oakland, CA, pp. 979-988, March 14-18, 1999.

Yang, X. and LaBrecque, D. 3-D stochastic inversion of ERT data, Proceeding of the SAGEEP, Chicago, IL, pp. 221-228, March 22-26, 1998.

Yeh, T.-C. J., D. LaBrecque, D. Alumbaugh, B. Li, and X. Yang, A stochastic hydrogeophysical joint inversion technique for monitoring movement of water and characterizing the vadose zone, AGU fall meeting 1997, San Francisco, CA.

Yeh,T-C. J., Alumbaugh, D., Liu, S. and Paprocki, L., A Stochastic HydroGeophysical Joint Inversion Technique for Monitoring and Characterizing the Vadose Zone, AGU fall meeting 1998, San Francisco, CA.

Technical Report

Brainard, J. R., Glass, R. J., Alumbaugh D. L., Paprocki, L., Labrecque, D. J., Yang, X., Yeh, T.-C. J., Baker, K, E., and Rautman, C. A., "The Sandia-Tech Vadose Zone Facility: Experimental Design and Data Report of a Constant Flux Infiltration Experiment", Sandia National Laboratories, Albuquerque, NM, Publication in Progress 2001.

Thesis' and Dissertations

Baker, K. E. Investigation of Direct and Indirect Laboratory Characterization Methods for Heterogeneous Alluvial Deposits: Application to the Sandia-Tech Vadose Zone Infiltration Test Site Masters Thesis, Department of Hydrology, New Mexico Institute of Mining and Technology, Socorro, NM, 2001.

Paprocki, L. T., Characterization of vadose zone in-situ moisture content and an advancing wetting front using cross-borehole ground penetrating radar; Masters Thesis, Department of Hydrology, New Mexico Institute of Mining and Technology, Socorro, NM, 2000.

Yang, X., Stochastic inversion of 3-D ERT data, Ph.D. dissertation, the University of Arizona, Dept. of Mining and Geological Engineering, Tucson, Arizona 1999.

8 Interactions:

Record interactions that stem from the research including the following:

a. participation/presentations at meetings, workshops, conferences, seminars, etc.

Investigators in the project also participated in the Advanced Vadose Zone Characterization Workshop at Hanford in January of 2000, and have been in contact with the Tank Focus Area about performing a similar test at the Hanford Reservation.

b. consultative and advisory functions to other laboratories and agencies, especially DOE and other government laboratories. Provide factual information about the subject matter, institutions, locations, dates, and name(s) of principal individuals involved.

Jim Yeh was invited to INEEL, Idaho Falls, Idaho for the summer of 1999 to collaborate with Dr. Annette Schafer to investigate reactive transport in the heterogeneous vadose zone**.**

Jim Yeh and Robert J. Glass have both served on several committees on for the DOE complex-wide vadose zone science and technology roadmap: characterization, modeling, and simulation of subsurface contaminant fate and transport.

c. Collaborations:

Jim Yeh was invited to INEEL, Idaho Falls, Idaho for the summer of 1999 to collaborate with Dr. Annette Schafer to investigate reactive transport in the heterogeneous vadose zone.

9 Transitions:

10 Patents:

A patent disclosure for the sequential, geostatistical inverse approach has been submitted to the University of Arizona and is in review.

11 Future Work:

a. What remains to be done? Will the project lead to future work? If so, describe the nature of the future work.

1. Quantify the spatial variability of geophysical, hydrologic, chemical and biological properties of geological materials from the laboratory scale to the basin scale, and identify relationships between the different types of properties. The variability and relationships then needs to be related to geological lithology and the deposition environment. The result of this exercise would be a predictive model for general variability a given type of alluvial deposit.

2. Investigate how to better deploy geophysical and hydrologic sources and sensors in a cost-effective yet optimal manner. This may involve the investigation of "network designs" and other experimental design methods to maximize measurement resolution while minimizing the cost.

4. Develop new types of geophysical interpretation schemes that consider variability, and incorporate other data such as hydrologic, geochemistry, and geophysical data, point measurements.

5. Hydrologic and geophysical modeling problems need to be resolved. Specific issues include accuracy of the model in representing the true-earth processes, and computational issues (speed, domain size, and resolution). Since all noninvasive approaches rely on inverse modeling, it is important to understand if the mathematical models adequately represent the true processes in the medium. We also need to develop computationally efficient inverse algorithms so that a geological basin can be characterized at high resolution within a reasonable time frame. Finally, we need to investigate methods for incorporating measurements at different scales into the inverse algorithms.

6. Innovative new sensors need to be developed that reduce cost.

7. Hydraulic/pneumatic/chemical noninvasive characterization methods need to be developed for detecting unsaturated flow. Also tracer tomography (soil and gas surveys) techniques need to be investigated.

8. Improve communication with, and the education of practitioners, clients, and regulators regarding advances in techniques and methods.

12 Literature Cited

Alumbaugh, D. L., Paprocki, L., Brainard, J., Glass, R.J., and Rautman, C., 2000, Estimating in-situ moisture contents using cross-borehole ground penetrating radar; a study of accuracy, repeatability and resolution, to be submitted to Water Resources Research.

Aldridge, D.F. and Oldenburg, D.W., 1993. Two-dimensional tomographic inversion with finite-difference travel times. Joural of Seismic Exploration, 2:257-274.

Archie, G.E., 1942 Electrical resistivity log as an aid in determining some reservoir characteristics, Am. Inst. Mining and Metal. (Engr. Transl.), 146, 54-62

Aki, K., and Richards, P.G., 1980, Quantitative seismology: theory, and methods, W. H. Freeman (Sand Francisco), 695-699.

Chan, T.F., Gallopoulos, E., Simoncini, V., Szeto, T., and Tong, C.H., 1994, A quasi-minimal residual variant of the Bi-CGSTAB algorithm for nonsymmetric systems, SIAM Journal on Scientific Computing, 15, No. 2, 338-347.

Hanna, S. and T.-C. J. Yeh, Estimation of co-conditional moments of transmissivity, hydraulic head, and velocity fields, *Adv. in Water Resou*r., 87-93, 22(1), 1998.

LaBrecque, D. J., Morelli, G., Daily W., Ramirez, A., and Lundegard, P., 1999, Occam's Inversion of 3D ERT data: in: Spies, B., (Ed.), Three-Dimensional Electromagnetics, SEG, Tulsa, 575-590.

Liedl, R., 1994. A conceptual perturbation model of water movement in stochastically heterogeneous soils. Adv. Water Resour. 17, 171-179.

Morelli, G., and LaBrecque, D. J., 1996, Robust scheme for ERT inverse modeling: European Journal of Environmental and Engineering Geophysics, 2, 1-14.

Russo, D. and M. Bouton, 1992. Statistical analysis of spatial variability in unsaturated flow parameters. Water Resour. Res. 28(7), 1911-1925.

Srivastava, R., and T.-C. J. Yeh, 1992. A three-dimensional numerical model for water flow and transport of chemically reactive solute through porous media under variably saturated conditions. Adv. Water Resour. 15(5), 275-287.

Tarantola, A., 1987, Inverse problem theory: Methods for data fitting and model parameter estimation, Elsevier

Topp, G.C., Davis, J. L. and Annan, A.P., 1980. Electromagnetic determination of soil water content: Measurement in coaxial transmission lines. Water Resources Research, 16(3):574-582.

van Genuchten, M. T., A closed-form equation for predicting the hydraulic conductivity of unsaturated soils. *Soil Sci. Soc. Am. J.* 44, 892-898, 1980.

Waxman, M.B. and Smith, L.J.M., 1968, Electrical conductivity in oil-bearing shaly sands, Soc. Petre. Engrs. J., 107-122.

Yeh, T.-C., M. Jin, and S. Hanna, An iterative stochastic inverse method: conditional effective transmissivity and hydraulic head fields, *Water Resour. Res.,* 32(1), 85-92, 1996.

Yang, X. and LaBrecque, D. J., 1999, Stochastic Inversion of 3D ERT data: Proceedings of the Symposium on the Application of Geophysics to Engineering and Environmental Problems, 221-228.

Zhang, J., R. l. Mackie, and T. Madden, 3-D resistivity forward modeling and inversion using conjugate gradients. *Geophysics 60,* 1313-1325, 1995.

Zhang, J., and T.-C. J. Yeh, 1997. An iterative geostatistical inverse method for steady flow in the vadose zone. Water Resour. Res. 33(1), 63-71.

13 Feedback

The bi-annual workshop needs to have a better focus and purpose, and that focus needs to be made apparent to the PI's. The focus of the first workshop was well defined- get the end users together with the investigators. The purpose of the second workshop was a bit of a mystery, as the end-users were not invited in general.